Turk J Chem
27 (2003) , 683 – 693.

Isolation and Characterization of a Smectite as a Micro-Mesoporous Material from a Bentonite

Müşerref ÖNAL[1], **Yüksel SARIKAYA**[1,*], **Tülay ALEMDAROĞLU**[1], **İhsan BOZDOĞAN**[2]
[1] *Ankara University, Faculty of Science, Department of Chemistry, Beşevler, 06100 Ankara-TURKEY*
e-mail: sakaya@science.ankara.edu.tr
[2] *Eczacıbaşı Ceramic Industries, Kısıklı Cad. 1, Altunizade, Üsküdar, 81190 İstanbul-TURKEY*

Received 19.03.2003

A procedure was assessed for obtaining an optimum amount of a micro-mesoporous material known as smectite from Reşadiye (Tokat/Turkey) bentonite. The procedure, which will permit a better economic evaluation of the Reşadiye reserves, is based on successive settlements of bentonite suspensions during various time intervals. To characterize the original bentonite, its fractions and the high purity smectite product, X-ray diffraction, differential thermal analysis, thermogravimetric analysis, scanning electron microscopy and nitrogen adsorption-desorption techniques were used. The original bentonite contained 50% by mass sodium-rich smectite (NaS) and 10% by mass NaCa-smectite (NaCaS). It also contained illite, clinoptilolite, analcime, feldspar, calcite, dolomite, quartz and opal-C. It was determined that the NaCaS particles were laminated whereas the NaS particles were delaminated. The specific surface areas of the original bentonite and NaS were respectively 27 m ^{2}g $^{-1}$ and 43 m ^{2}g $^{-1}$ and the specific micropore-mesopore volumes were respectively 0.055 cm ^{3}g $^{-1}$ and 0.065 cm ^{3} g $^{-1}$. It was established that the porosity increased after purification. It was concluded that it was possible to isolate a micro-mesoporous material, i.e. high purity NaS, with a yield of 50% from the aqueous suspension of bentonite. The procedure did not require the use of any chemical reagent.

Key Words: Bentonite, mineralogy, porosity, purification, smectite, suspension.

Introduction

Bentonites have a wide spectrum of application areas[1−3]. They are either used directly or after treatment. For example, in areas such as the preparation of drilling fluids, pelletizing iron ores, the casting industry, purification of discharge waters, building applications and pet litter production, bentonites are used directly[4,5] whereas for the bleaching of edible oils acid activated bentonites are used[6−10]. Smectites are the major minerals in bentonites. In addition, some nonclay minerals and other clay minerals are contained in bentonites.

*Corresponding author

The quality and characteristics of a bentonite depend largely on the quality and quantity of the smectite, which is a micro-mesoporous material.

High purity smectites obtained by the purification of bentonites are used in a wide variety of areas such as carbonless copy paper[11], selective adsorbent[12–14], medication[15–17], membrane[18], organoclay[19–21], polymeric clay[22], pillared clay[23–25], nanoclay[26] and catalyst[27] production. Therefore, the isolation of some smectite group minerals from bentonites is of great importance. Some of these minerals that are porous materials are montmorillonite, beidellite, nontronite, saponite and hectorite. Nevertheless, no definite procedure exists for the isolation of these porous materials from bentonites. A specific purification method for each bentonite needs to be developed depending upon the properties of its clay and nonclay minerals. A unit layer of smectite minerals (TOT, 2:1) is formed by the bonding through oxygen bridges of 1 alumina sheet composed of octahedrons [O: $AlO_3(OH)_3^{6-}$] between 2 silica sheets composed of tetrahedrons [T: SiO_4^{4-}]. Smectite powders are formed by the agglomeration of TOT layers whose thicknesses vary between 0.96 and 1.50 nm and whose widths vary between tens to hundreds of nanometers. The particle sizes of these agglomerated smectite particles are smaller than 2 μm in aqueous suspensions. This property is of great importance in the purification of bentonites since it permits the separation of smectites from the bentonites.

The objective of this study was to isolate as pure a smectite as possible from a bentonite and to determine some physicochemical properties of the original bentonite, intermediate fractions and isolated smectite.

Materials and methods

The Reşadiye (Tokat/Turkey) bentonite bed is one of the largest sodium bentonite (NaB) reserves in Turkey. Its potential reserves have been estimated at 200 million t by the Mineral Research and Exploration Institute of Turkey. This bentonite produces muds of high plasticity when mixed with water. It is currently used in the preparation of drilling fluids and in iron ore pelletizing. A yellowish-green bentonite taken from this bed was chosen as the material for this study.

In the light of the colloidal properties of aqueous bentonite suspensions, the following steps were taken for the assessment of a suitable procedure for the isolation of smectite from the bentonite.

The original sample was ground to pass through a screen with a clear opening of 0.074 mm. The ground sample was dried at 105 °C for 4 h, labeled as RT and stored.

A suspension was prepared by adding 10 g of RT sample to 0.5 L of distilled water at room temperature. This was continuously stirred by a magnetic stirrer for 2 h and then left. An orange fraction (F1) precipitated in 15 min in this first system and the suspension on top was transferred to another flask by siphoning. F1 was washed with distilled water, which was added to the previously separated suspension. The volume of the suspension was adjusted to 0.5 L, stirred for 2 h and then left . A white fraction (F2) precipitated in 3 days in this second system. The former procedure, beginning with the siphoning of the suspension, was repeated and a third fraction (F3) that precipitated in 1 week in the third system was obtained. Repetition once more of the same procedure did not result in the production of a precipitate in 1 month (which is taken as an infinite period) in this fourth system. A yellowish-green fraction (F4) was obtained by the evaporation of the water contained in the suspension. The above purification processes were repeated until a total of 2 kg of fraction F4 had been obtained. The total obtained F1, F2, F3 and F4 fractions were dried at 105 °C for 4 h, weighed and stored for subsequent experiments.

The original bentonite and its fractions were kept at 1000 °C for 2 h and their losses on ignition (LOI) were determined. The chemical analyses (CA) of these samples were performed by a Hitachi Z-8200 atomic absorption spectrophotometer. The cation exchange capacities (CEC) defined as the equivalent amount of exchangeable cations in 1 kg of each sample, were determined according to the methylene blue procedure[28,29]. The methylene blue was supplied by the Merck Chemical Company.

For X-ray determinations, aqueous suspensions of the original bentonite (RT) and its fractions (F1-F4) were prepared. The suspensions were filtered under vacuum and the precipitates obtained were air dried. The X-ray diffraction (XRD) patterns of the samples were determined by a Philips PW 1730 diffractometer in which CuK_{α}X-rays and a nickel filter were used. A randomly oriented mount[30] was used for XRD determinations.

The volumetric particle size distribution (PSD) curves and particle outer surface areas (S) of RT, F1, F2, F3 and F4 samples were determined by a mastersizer (Malvern Instruments Model Micron) instrument. The differential thermal analysis (DTA) and thermalgravimetric analysis (TGA) curves of the same samples were determined by a Netzsch Simultaneous TG-DTG-DTA instrument (Model 429) at a heating rate of 10 K min $^{-1}$ and α-Al_2O_3 was used as an inert material during the determinations. The same samples were investigated by a scanning electron microscope (SEM, LEO-453). The adsorption and desorption isotherms at liquid nitrogen temperature of the same samples were also determined. A volumetric adsorption instrument made of Pyrex glass and connected to a high vacuum was used in the experiments[31,32].

Results and Discussion

Mineralogy

The XRD patterns of RT and its fractions are shown in Figure 1. The XRD results were compared with those in the literature[30] and it was determined that RT contained clay minerals such as sodium-rich smectite (NaS), sodium-calcium smectite (NaCaS) and illite (I). The $d(001)$ values of NaS and NaCaS were calculated respectively as 1.21 nm and 1.38 nm by the Bragg equation. From the positions and intensities of the smectite peaks in the XRD patterns it was decided that the major clay mineral was NaS. From the XRD patterns, it was clearly observed that F4 fraction was high purity NaS. A detailed examination of XRD patterns showed that RT contained clinoptilolite (Cln), analcime (An), feldspar (F), calcite (C), dolomite (D), quartz (Q) and opal-C (OC) as non clay minerals.

The settling times of the fractions and their mass percents (mass % F) determined by weighing as well as the CECs and CAs of all the samples are presented in Table 1. The CEC may be considered to be approximately equal to the molar surface charge. It can be assumed that the CECs determined by the methylene blue procedure originate from clay minerals, and more specifically from smectites, since the CECs of clay minerals such as illites as well as zeolites and other nonclay minerals are so small that they may be considered negligible. Accordingly, the respective ratios of the CEC values of RT, F1, F2 and F3 to the CEC value of F4, that is pure NaS, were multiplied by 100 to obtain the respective mass percents of smectites (mass % S). The obtained results are presented in Table 1. The mass percents of smectites in each fraction in the original bentonite were calculated by the equation: mass % S in RT = (mass % F) x (mass % S), and are presented in Table 1. The total amount of smectites in RT was established directly as 60%. It was also calculated by taking the sum of the amount of smectites found in each fraction, which was 58.8 %. It

was observed that there was a good correspondence between these 2 values. It was decided that the original bentonite that contained mostly NaS was a sodium bentonite, and it was labeled RT (NaB).

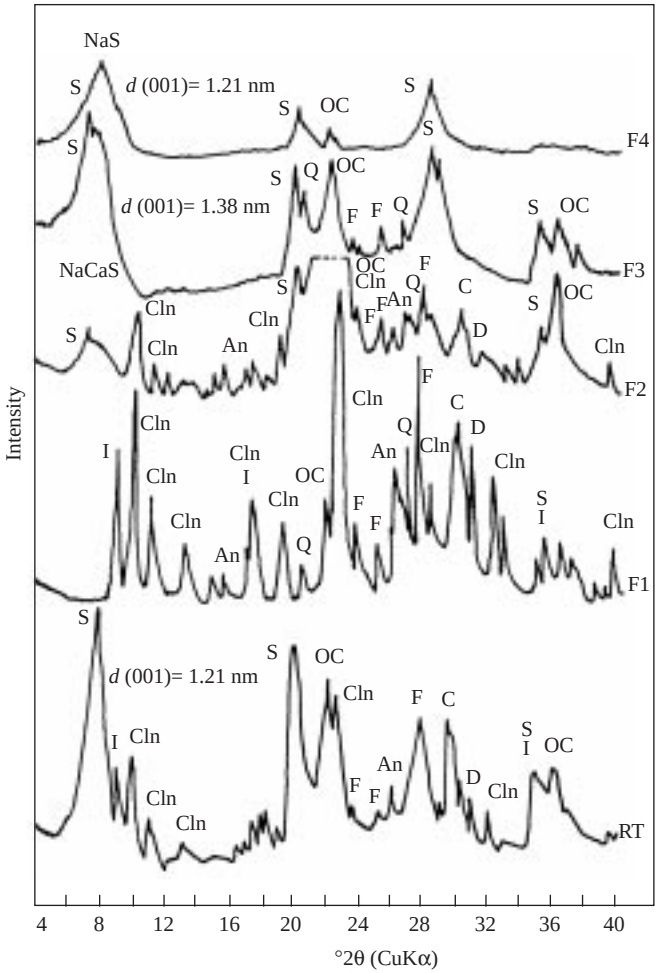

Figure 1. The XRD patterns of the original bentonite and its fractions (An: Analcime, C: Calcite, Cln: Clinoptilolite, D: Dolomite, F: Feldspar, I: Illite, OC: Opal-C, Q: Quartz, S: Smectite).

The DTA and TGA curves of the original bentonite and its fractions are shown in Figures 2 and 3, respectively. On these curves, the endothermic reactions labeled *a*, *b* and *c* represent dehydrations, dehydroxylations and calcinations, respectively. On the DTA curves the exothermic transformations labeled *d* represent recrystallizations. Since no mass change occurs during recrystallization no change due to recrystallization appears on the TGA curves. The volumetric PSD curves of the same samples plotted as *d(Vol %)/ dD – D* are shown in Figure 4. The $D < 2\mu$m portions of these curves show the PSD of clay minerals, especially smectite minerals, since only clay minerals can disperse below 2 μm in aqueous suspensions. The particle sizes of nonclay minerals are generally larger than 2 μm. This difference makes the separation of clay minerals from nonclay minerals easier.

Table 1. Some physicochemical properties of the original bentonite and its fractions.

Properties of Samples	RT(NaB)	F1	F2	F3	F4(NaS)
Precipitation time	-	15 min	3 days	1week	∞
Mass % F	100	25	18	7	50
CEC (eqv kg^{-1})	0.65	0.02	0.21	0.75	1.08
Mass % S	(60)	1.8	19.4	70	~ 100
Mass % S in RT	58.8	0.5	3.5	4.8	50
Chemical Analyses					
SiO_2	62.60	55.25	75.05	65.40	61.97
TiO_2	0.29	0.18	0.83	0.74	0.22
Al_2O_3	16.65	13.55	10.40	16.65	19.73
Fe_2O_3	3.44	1.11	1.49	3.97	4.74
MgO	1.63	0.85	0.79	1.69	2.40
CaO	3.37	9.83	2.17	0.78	0.91
Na_2O	2.59	3.11	1.59	1.75	2.58
K_2O	0.98	3.03	1.69	0.49	0.38
LOI	8.45	12.90	5.85	6.30	7.08

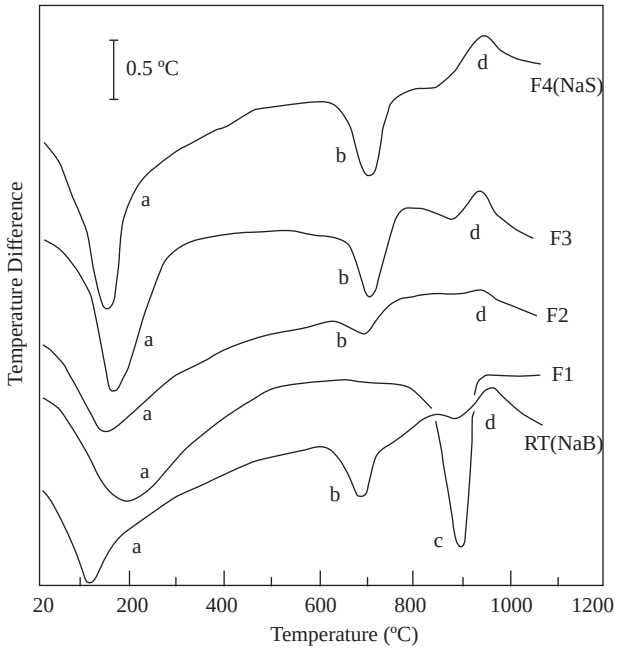

Figure 2. The DTA curves of the original bentonite and its fractions (a: Dehydration, b: Dehydroxylation, c: Calcination, d: Recrystallization).

According to the above XRD, CEC, CA, DTA, TGA and PSD data the distribution of clay and nonclay minerals among the different fractions can be discussed as follows. The total I as well as large amounts of Cln, An, F, OC, Q, C and D were separated by settlement in F1. The amount of smectite minerals in F1 was so small that it may be considered negligible. Most of the remaining Cln, An, F, OC, Q, C and D were separated by settlement in F2. It was determined that a small amount of NaCaS was present in F2, which contained a rather high amount of OC. A small amount of Q, OC and F were present in F3

whose major clay mineral was NaCaS. It was observed that F4 which contained a trace amount of OC, was almost pure NaS. From the CA results of F4, the structural formula[33] of NaS was determined as follows:

$Na_{0.319}K_{0.031}\ Ca_{0.062}\ (Al_{1.511}\ Mg_{0.229}Fe^{2+}_{0.222}\ Fe_{0.006}Ti_{0.011})(Si_{3.966}Al_{0.034})O_{10}(OH_2).nH_2O$

This formula showed that NaS was very similar to the sodium-rich mineral montmorillonite (NaM).

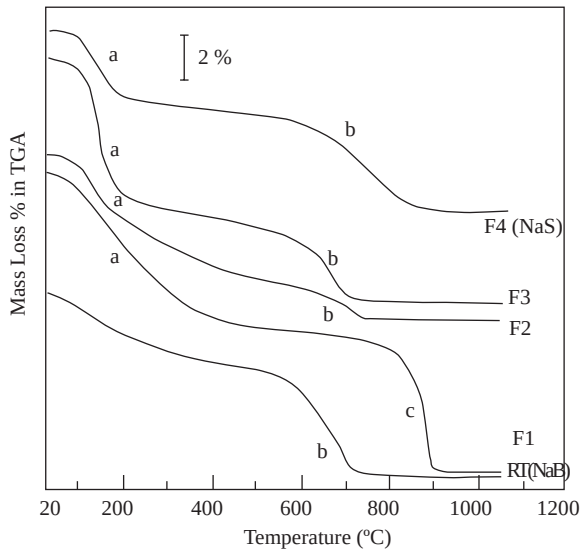

Figure 3. The TGA curves of the original bentonite and its fractions (a: Dehydration, b: Dehydroxylation, c: Calcination).

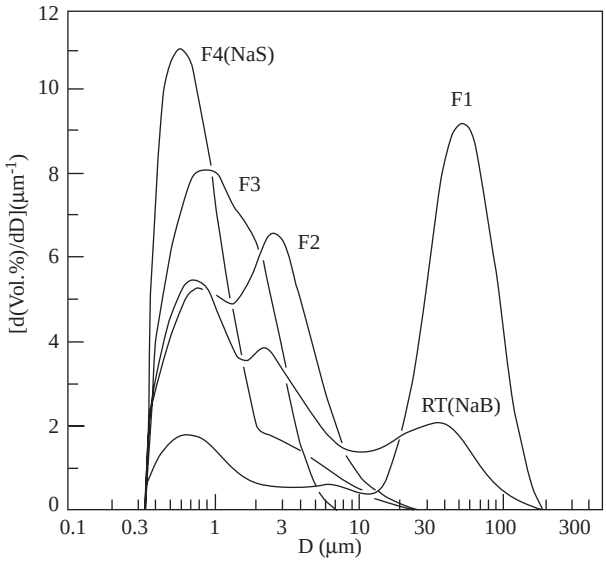

Figure 4. The PSD curves of the original bentonite and its fractions.

The SEM photograph of NaCaS obtained as a result of successive settlements from aqueous suspensions by the separation of nonclay minerals is shown in Figure 5. The laminated structure shows that there are surface-surface interactions between the particles. The SEM photograph of NaS that was left in F4 is shown in Figure 6. The delaminated structure shows that there are edge-edge and edge-surface interactions between the particles. Therefore, cylindrical agglomerates were formed.

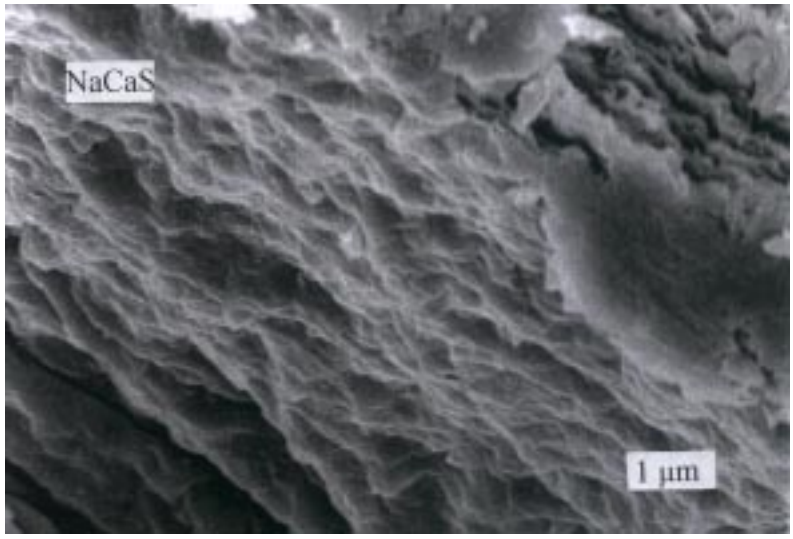

Figure 5. A SEM photograph of the laminated NaCaS mineral contained in the F3 fraction.

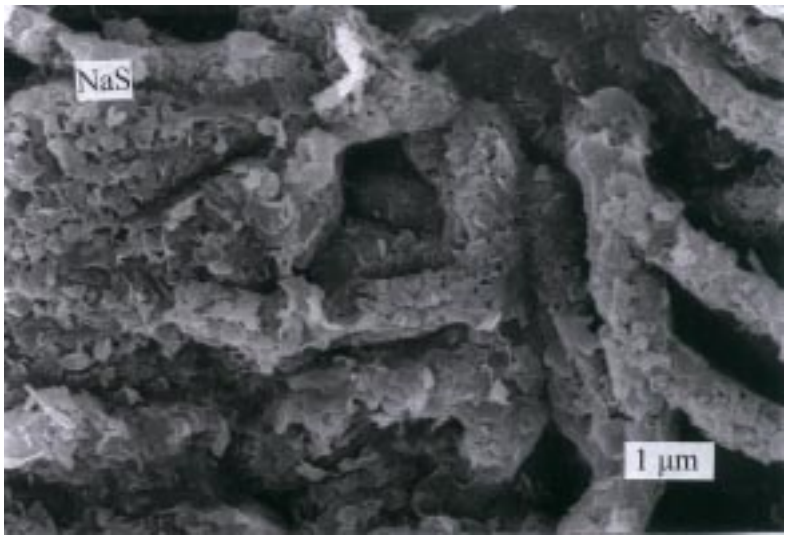

Figure 6. A SEM photograph of the highest purity delaminated NaS mineral that comprises the F4 fraction.

Adsorptive properties

In the SEM photographs of NaCaS and NaS respectively shown in Figures 5 and 6 respectively, the macropores whose widths are larger than 50 nm are observed whereas, the micropores whose widths are smaller than 2 nm and mesopores whose widths vary between 2 nm and 50 nm are not observed. The contribution of macropores to the adsorptive properties may be considered negligible compared to the contribution of micro- and mesopores. Micro- and mesoporous structure is generally investigated by the adsorption and desorption of nitrogen.

Among the adsorption-desorption isotherms of nitrogen at 77 K that were determined for the original bentonite and its fractions, those belonging to RT (NaB) and F4 (NaS) samples were chosen to be shown in Figure 7. Here, p represents the adsorption equilibrium pressure, p^0 represents the vapor pressure of bulk liquid nitrogen at experimental temperature and $p/p^0 \equiv x$ represents the relative equilibrium pressure. The adsorption capacity, defined as the molar amount of nitrogen adsorbed on 1 g of adsorbant at any

x, is represented by n. The isotherms of RT and F4 presented in Figure 7 show that adsorption capacity increases with purification. The specific surface areas (A) of RT and its fractions determined according to the Brunauer, Emmett and Teller[34] procedure by using the adsorption data are listed in Table 2. The outer surface areas (S) of the particles determined by the light scattering of particles during PSD determinations are also presented in Table 2. It was observed that the S values were rather small compared to the BET values resulting from the pore walls inside the particles. A comparison of the results presented in Table 2 showed that the A and S values increased as the mass percents of smectites in the fractions increased.

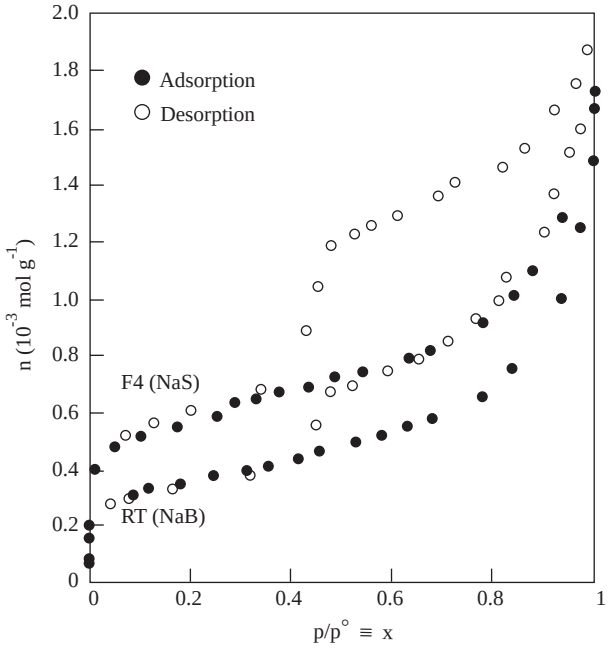

Figure 7. The isotherms of the adsorption and desorption of nitrogen at 77 K on the RT (NaB) and F4 (NaS).

Table 2. The specific surface areas (A), specific outer surface areas (S) and specific micropore-mesopore volumes (V) of the original bentonite and its fractions.

	RT(NaB)	F1	F2	F3	F4(NaS)
A (m^2g^{-1})	27	5	24	38	43
S (m^2g^{-1})	4.6	1.5	4.8	6.4	7.8
V (cm^3g^{-1})	0.055	0.030	0.070	0.055	0.065

The adsorption capacity, which was determined from the desorption isotherm as the liquid nitrogen volume at every p/p^0 was taken as the specific pore volume (V). At these p/p^0 values, the capillary radii were calculated by using the corrected Kelvin equation[35]. The $V - r$ pore size distribution curves of RT (NaB) and F4 (NaS) samples are shown in Figure 8. The values of V at $r = 25$ nm were taken as specific micropore-mesopore volumes, as already explained in our previous studies[36–39]. The values of those pore volumes are given in Table 2. The mesopore size distribution curves $(dV/dr) - r$ of RT and F4 are presented as examples in Figure 9. It was observed that the mesopore radii, and especially the average mesopore radius, did not change appreciably, whereas the number of mesopores increased considerably with purification.

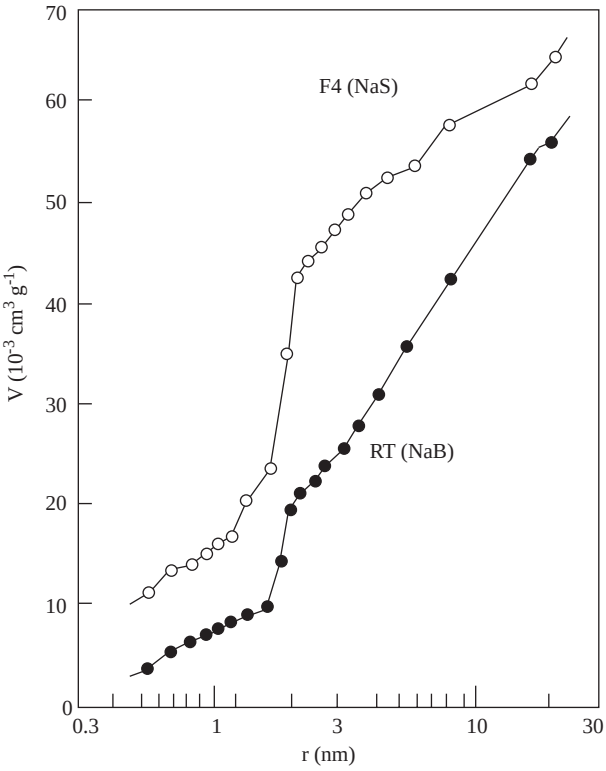

Figure 8. The mesopore size distribution curves ($V - r$) for RT (NaB) and F4 (NaS) samples.

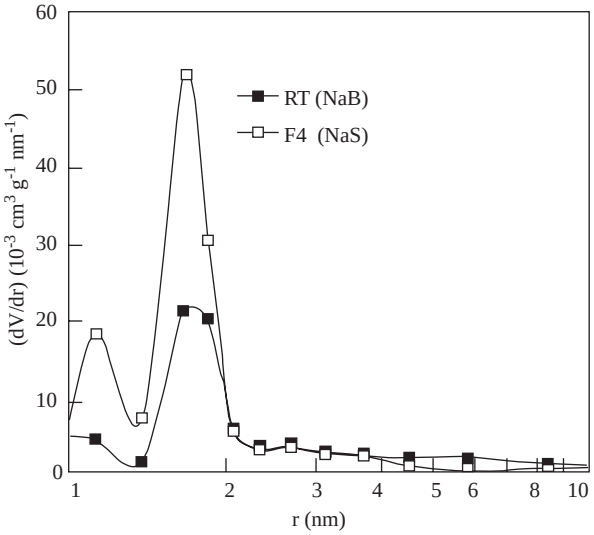

Figure 9. The mesopore size distribution curves (dV/dr-r) for RT (NaB) and F4 (NaS) samples.

Conclusion

The characterization studies showed that the procedure followed which was based on successive settlements of bentonite suspensions during various time intervals, was successful at isolating the micro-mesoporous material known as smectite. A NaS mineral that was similar to NaM and that contained a trace amount of opal-C was isolated from the aqueous suspension of bentonite with a yield of 50%. It was observed that the densities and particle size distributions of nonclay minerals were effective during the settlement and

siphoning processes of the aqueous suspension. Since the procedure followed does not require the use of any chemical reagent, it will permit a better economic evaluation of bentonite in wider application areas such as carbonless copy paper, selective adsorbent, medication, membrane, organoclay, pillared clay, nanoclay and catalyst production, in which high purity smectites are used as micro-mesoporous materials.

Acknowledgments

The authors thank the Scientific and Technical Research Council of Turkey TÜBİTAK for supporting this work under project TBAG-1986 (100T101).

References

1 R.E. Grim and N. Güven**, Bentonites, Geology, Mineralogy, Properties and Uses, Developments in Sedimentology,** Volume 24, Elsevier, Amsterdam, 1978.

2 H.H. Murray, **Appl. Clay Sci. 5,** 379-395 (1991).

3 H.H. Murray, **Appl. Clay Sci. 34**, 39-49 (1999).

4 T.A. Wolfe, T. Demirel and E.R. Baumann, **Clay. Clay Miner. 33**, 301-311 (1985).

5 M. Kovalska, H. Güler and D.L. Cocke, **Sci. Total Environ. 141**, 223-240 (1994).

6 T.L. Mounts, **J. Am. Oil Chem. Soc. 58**, 51A-54A (1981).

7 E. Srasra, F. Bergaya, H. Van Damme and N.K. Ariquib, **Appl. Clay Sci. 4**, 411-421 (1989).

8 E. Gonzalez-Paradas, M. Villafrance-Sanchez and A. Gallego-Campo, **J. Chem. Tech. Biotech. 57**, 213-216 (1993).

9 P. Falaras, I. Kovanis, F. Lezou and G. Seiragakis, **Clay Miner. 34**, 221-232 (1999).

10 M. Önal, Y. Sarıkaya, T. Alemdaroğlu and İ. Bozdoğan, **Turk. J. Chem. 26**, 409-416 (2002).

11 M. Takashima, S. Sano and S. Ohara, **J. Imag. Sci. Tech. 37**, 163-166 (1993).

12 H. Ceylan, A. Yıldız and Y. Sarıkaya, **Turk. J. Chem. 17**, 267-272 (1993).

13 R.M. Barrer, **Clay. Clay Miner. 37**, 385-395 (1989).

14 A. Pusino, I. Braschi and C. Gessa, **Clay. Clay Miner. 48**, 19-25 (2000).

15 H. Robert, S. Robertson and R.M. Ward, **J. Phar. Pharmacol. 3**, 27-35 (1951).

16 E. Gomiz, J. Linares and R. Delgado, **Appl. Clay Sci. 6**, 359-368 (1992).

17 R. Bolgar, **Ind. Miner. August**, 52-63 (1995).

18 S.T. Fritz, **Clay. Clay Miner. 34**, 214-223 (1986).

19 G. Lagaly, **Philos. Trans. Roy. Soc. London, A311**, 315-332 (1984).

20 C. Breen, R. Watson, J. Mandejova, P. Komadel and Z. Klapyta, **Langmuir 13**, 6473-6479 (1997).

21 G. Sheng and S.A. Boyd, **Clay. Clay Miner. 48**, 43-50 (2000).

22 P. F. Luckham and S. Rossi, **Adv. Coll. Interf. Sci. 82**, 43-50 (1999).

23 M. Sychev, R. Prihod'ko, A. Stepanenko, M. Rozwadowski, V.H.J. De Beer and R.A. Van Santen, **Microporous Mesoporous Mater. 47**, 311-321 (2001).

24 J.M. Guil, J.A. Perdigon-Melon, M. Brotas de Carvalho, A.P. Carvalho and J. Pires, **Microporous Mesoporous Mater. 51**, 145-154 (2002).

25 J.L. Valverde, P. Sanchez, F. Dorado, C.B. Molina and A. Romero, **Microporous Mesoporous Mater. 54**, 155-165 (2002).

26 J. Quarmley and A. Rossi, **Ind. Miner. January**, 47-53 (2001).

27 F. Kooli and W. Jones, **Clay Miner. 32**, 633-643 (1997).

28 G. Rytwo, C. Serben, S. Nir and L. Margulies, **Clay. Clay Miner. 39**, 551-555 (1991).

29 C.H. Yu, S.Q. Newton, M.A. Norman, D.M. Miller, L. Schafer and B. J. Teppen, **Clay. Clay Miner. 48**, 665-671 (2000).

30 D.M. Moore and R.C. Reynolds, **X-ray Diffraction and the Identification and Analysis of Clay Minerals**, 2nd ed., Oxford University Press, Oxford 1997.

31 Y. Sarıkaya and S. Aybar, **Commun. Fac. Sci. Uni. Ank. B24**, 33-39 (1978).

32 M. Önal, Y. Sarıkaya and T. Alemdaroğlu, **Turk. J. Chem. 25**, 241-249 (2001).

33 A.C.D. Newman and G. Brown, **The Chemical Constitution of Clays. In: Chemistry of Clays and Clay Minerals** (Newman, A.C.D. Editor) Monograph No. 6, Mineralogical Society, London, pp. 1-128, 1987.

34 S. Brunauer, P.H. Emmett and E.J. Teller, **J. Am. Chem. Soc. 60**, 309-319 (1938).

35 S. Gregg and K.S.W. Sing, **Adsorption Surface Area and Porosity**, Academic Press, London, 1982.

36 İ. Sevinç, Y. Sarıkaya and M. Akınç, **Ceram. Inter. 17**, 1-4 (1991).

37 Y. Sarıkaya, M. Önal, B. Baran and T. Alemdaroğlu, **Clay. Clay Miner.** 48, 557-562 (2000).

38 Y. Sarıkaya, İ. Sevinç and M. Akınç, **Powder Tech. 116**, 109-114 (2001).

39 Y. Sarıkaya, T. Alemdaroğlu and M. Önal, **J. Eur. Cer. Soc. 22**, 305-309 (2002).